INFLUENCE OF CARBON FIBRES ON THE CRYSTALLINITY OF POLYAMIDE-6

Thomas Guglhoer, Marco Korkisch and Markus G. R. Sause

Experimental Physics II, Institute of Physics, University of Augsburg
Universitätsstrasse 1, D-86135 Augsburg, Germany
Email: thomas.guglhoer@physik.uni-augsburg.de

Keywords: Polyamide-6, polymorphism, crystallinity

ABSTRACT

The influence of carbon fibres on the crystallinity of Polyamide-6 was investigated in dependence of the cooling rate during crystallization. Therefore, X-ray diffraction profiles were recorded layer by layer from end quench test samples of Polyamide-6 and carbon fibre reinforced Polyamide-6. The formation of α-phase and γ-phase was quantified as function of the measurement depth and were correlated to the cooling rates estimated from the heat diffusion equation. With and without fibre reinforcements the results show a γ-phase dominated surface layer and a α-phase rich bulk structure. The presence of carbon fibres was found to increase the thickness of the surface layer and the amount of γ-phase.

1 INTRODUCTION

For processing of carbon fibre reinforced thermoplastics, thermoforming above the melting temperature of the polymer is a common technique. One approach to reduce process cycle times is an increase in cooling rate after the thermoforming process. Nevertheless, the temperature profile during crystallization of semicrystalline thermoplastics is critical for the formation of crystalline structures and thus the thermomechanical properties of the polymer.

A critical aspect of understanding these processing-structure-property relationship of carbon fibre reinforced Polyamide-6 (CF/PA6) is the influence of carbon fibres on the development of microstructure within the matrix. Polyamide-6 (PA6) is a member of the family of semi-crystalline polymers and its microstructure consist of amorphous and crystalline regions. The crystalline fraction shows two polymorphs, typically referred to as α- and γ-phase. Both polymorphs crystallize under different thermal conditions and show different mechanical and thermomechanical properties.

The α-phase of PA6 is the thermodynamically most stable form. It shows an equilibrium melting temperature of 260°C [1] and a specific heat of fusion of 241 J/g [2]. Chain segments are fully extended and hydrogen bounds locate within the same plane [3]. The α-phase is obtained from the liquid state by slow cooling [4, 5] or isothermal crystallization at temperatures above 190°C [6]. At low crystallization temperatures or high cooling rates the γ-phase is the preferred crystalline phase. It is a metastable form which converts under annealing conditions into α-phase [7]. It has extended chain segments but its hydrogen bonds are not restricted to a single plane [3]. At cooling rates above 100 K/s [5] – 150 K/s [8] crystallization does not occur and PA6 remains in amorphous state.

The mechanical properties of both polymorphs differ with respect to their modulus, hardness and fracture behaviour. The α-phase shows a higher modulus [9] and hardness [10] whereas the γ-phase shows ductile failure behaviour [11].

The modulus of Polyamide-6 in general can be improved substantially by reinforcing carbon fibres. Beside the properties of Polyamide-6 and carbon fibres, the interaction between both constituents defines the macroscopic properties of the composite. It is well known from literature, that carbon fibres may influence the crystallization of semi-crystalline polymers because they act as nucleation sites [7, 12]. The nucleation at carbon fibres may lead to transcrystalline layers as shown by Bessel for Polyamid-6 [14]. As shown by Fornes [15] for clay/Polyamide-6 and by Feng [16] for CF/PA6 the effect of nucleation sites depend strongly on nucleation site density and crystallization conditions. High nucleus concentration may hinder the crystallization process or induce phase selective crystallization.

Purpose of this study is to investigate the crystallinity as function of the cooling rate in PA6 and its carbon fibre reinforced composite. Therefore, PA6 and CF/PA6 samples are quenched from the liquid state and their crystallinity is determined using X-ray diffraction (XRD). The local cooling rates are estimated solving the heat diffusion equation.

2 EXPERIMENTAL

2.1 Material and sample preparation

Polyamide-6 (PA6) and carbon fibre reinforced Polyamide-6 (CF/PA6) samples were prepared using Polyamide-6 pellets supplied by Sigma Aldrich. The pellets were dried at least for 24h at 80°C in vacuum before processing. Carbon fibres (Sigrafil C30T050 EPY) supplied by SGL Carbon were used in a unidirectional layup for the CF/PA6 samples.

The PA6 sample was prepared melting the PA6 pellets in an aluminium foil box at 235°C in nitrogen environment. Subsequently, one side of the molten sample was cooled using a -18°C cold steel plate. This side will be further addressed as quenched side. The other side was insulated by a 1mm copper plate and cooled to ambient temperature in air (normal conditions).

Carbon fibres were impregnated with PA6 using a heating press at 235°C and a pressure of 1bar. The so obtained fibre reinforced laminates were quenched as described above for the PA6 sample.

For XRD measurements the samples were embedded in cold-setting epoxy resin. The samples were grinded gradually from the quenched side to collect an X-ray diffraction depth profile.

2.2 X-ray Diffraction

X-ray diffraction measurements have been performed using a Seifert XRD 3003 TT powder diffractometer with Ni-filtered Cu-Kα radiation. The diffraction profiles were collected in steps of 0.02° between 5° and 45° using a Meteor1D detector.

A multi-parameter fit procedure was applied to separate the contributions of α-, γ- and amorphous phase of PA6 from the diffraction profiles. Therefore, peak functions (Pearson-VII) for α_1, α_2, γ, and an amorphous peak were fitted to the diffraction profiles of PA6 using the Levenberg-Marquardt algorithm. An additional peak representing the contribution of carbon fibres was added in case of CF/PA6. The peak shape representing carbon fibres was obtained from a measured diffraction profile of neat carbon fibres under identical conditions as for the laminate.

The phase fractions of α-, γ- and amorphous phase was evaluated using the relative peak areas. Typical results for the fitting procedure are shown in Fig. 1(a) for PA6 and Fig. 1(b) for CF/PA6, respectively.

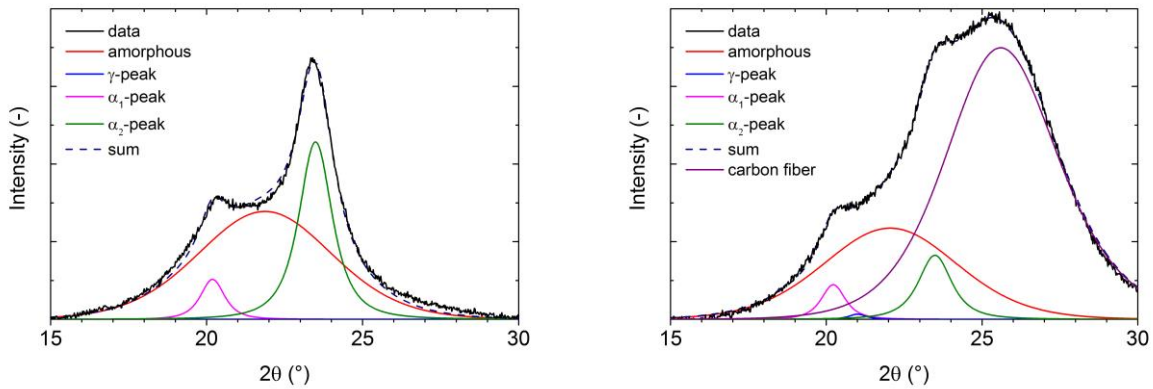

(a) PA6 (b) CF/PA6

Figure 1: Result of multi-parameter fit procedure for quantification of individual phases from diffraction profiles.

3 RESULTS

3.1 Depth profiles

Diffraction profiles of PA6 are shown in Fig. 2(a) for different measurement depths, whereas the depths are measured relative to the quenched surface. All diffraction profiles show a broad peak at 21.5°, which represents the amorphous contribution. With increasing measurement depth a growing contribution of a peak at 21.2° can be observed, which overlays the amorphous peak. This peak is related to the γ-phase. At a measurement depth of 0.63 mm the appearance of a shoulder at around 23° indicates the presence of the α-phase. At a measurement depth of 1.91 mm the diffraction profile is dominated by a two-peak structure, which is typical for a sample with high α-phase fraction.

The results from the fitting procedure of the XRD profiles are shown in Fig. 2(b). As expected the amorphous phase fraction is at its maximum at the quenched surface. The amorphous fraction decreases gradually with increasing measurement depth from 95% to 64% at 1.91 mm. Up to ca. 700 µm the γ-phase is the dominating crystalline phase with a maximum fraction of 8%. Afterwards the α-phase starts to dominate and replaces the γ-phase completely at a depth of ca. 1 mm. The phase fraction increases up to 36% at the maximum measurement depth of 1.91 mm.

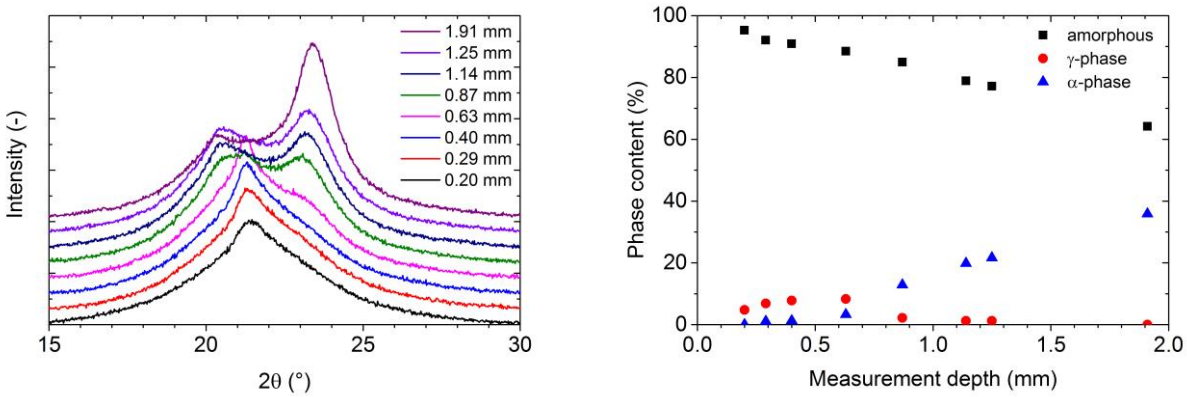

(a) diffraction profiles of PA6 (b) phase fractions of PA6

Figure 2: Diffraction profiles and phase fraction of the PA6 sample as function of the measurement depth.

Fig. 3(a) shows the diffraction profiles of CF/PA6. In comparison to the diffraction profiles of the pure PA6 an additional peak at 25.3° can be observed which indicates the presence of carbon fibres. Apparently the intensity of the carbon fibre peaks varies with measurement depth. This indicates a varying fibre volume fraction which has its minimum at 0.9-1.1 mm. The dominating carbon fibre peak is superimposed by the PA6 peaks. In analogy to the PA6 sample one can observe a peak at 21.3°, which indicates a presence of γ-phase at low measurement depth and a two-peak structure with increasing measurement depth which indicates a development of the α-phase.

The analysis of the diffraction profiles reveals a similar behaviour of CF/PA6 as found for the pure PA6: the amorphous phase fraction decreases gradually with increasing measurement depth from 95% to a minimum of 86% at a maximum measurement depth of 2.08 mm. The predominant crystalline phase up to 1.9 mm is the γ-phase with a maximum phase fraction of 15% at a measurement depth of 1.49 mm. In the core region of the sample the α-phase fraction replaces the γ-phase and is predominantly found at a depth of 2.08 mm.

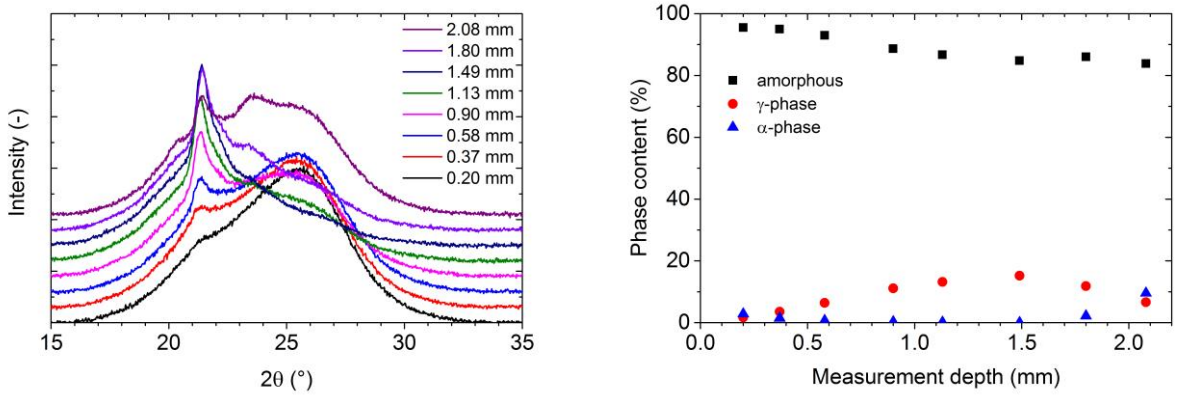

(a) diffraction profiles CF/PA6 (b) phase content CF/PA6

Figure 3: Diffraction profiles and phase fraction of the CF/PA6 sample as function of the measurement depth.

In contrast to earlier studies of Brucato et al. [4] the amorphous fraction shows a maximum at the surface of the sample. This indicates the effectiveness of the cooling mechanism. In addition, a nucleating effect of the steel plate surface can be excluded. The development of a γ-phase at the surface of PA6 samples is well known from injection-molding. Murthy et al. [17] describe the transition from γ-phase to α-phase at the surface and refer to it as skin-core morphology. Depending on the processing conditions the skin layer may have a thickness up to 1 mm. The skin layer in the prepared PA6 sample has a thickness of ca. 700 µm, whereas CF/PA6 shows a thickness of ca. 2.0 mm.

3.2 Cooling rate dependence

To estimate the cooling rates as function of the measurement depth the heat equation was solved numerically in 1D according to the boundary conditions used in the sample preparation. An overview of the geometrical configuration and the involved temperatures is given in Fig.4. The material properties used are reported in Table 1. It is noteworthy that the thermal conductivity of unidirectional CF/PA6 is highly anisotropic and, therefore, the conductivity perpendicular to the fibre direction was used as estimation for the present configuration (cf. Fig. 4). Perfect thermal contact between sample and copper was assumed and the heat of crystallization was neglected.

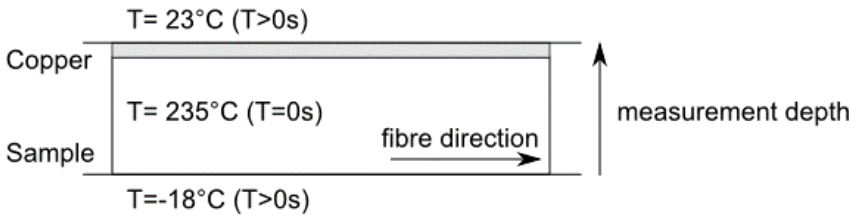

Figure 4: Boundary conditions for cooling rate estimation

Fig. 5 shows the estimated temperature profiles at the measurement depths for PA6 and CF/PA6, respectively. The cooling rates inside the CF/PA6 sample are higher compared to the PA6 sample, due to an increased thermal conductivity of CF/PA6 compared to PA6. Following the example of Brucato [18] and Cavallo [5] cooling rates at specific measurement depths are determined for a temperature of 135°C. For the present experimental setup, we expect a cooling rate in the range between 2.8 K/s and 180 K/s in case of PA6, and between 12 K/s and 1000 K/s in case of CF/PA6.

Material property		PA6	CF/PA6	Copper
Heat capacity	[J/kg/K]	1700	1070	385
Density	[kg/m³]	1150	1345	8700
Thermal conductivity	[W/m/K]	0.25	1.0	400

Table 1: Material properties used for cooling rate estimation.

Fig. 6 (a) shows the crystallinity of PA6 in dependence of the estimated cooling rates. At cooling rates below 20 K/s the α-phase dominates. Maximum phase fraction is 36% at a cooling rate of 2.8 K/s but a plateau is not reached, yet. At cooling rates above 15 K/s the contribution of the γ-phase increases and reaches its maximum value at a cooling rate of 30 K/min. A pure amorphous layer is not generated with cooling rates up to 180 K/s. In comparison the phase contents of CF/PA6 is shown in Fig. 6 (b). At cooling rates below 12 K/s most of the crystalline fraction contributes to the α-phase. At higher cooling rates γ-phase is the preferred crystalline fraction. The γ-phase shows a maximum content of 18% at a cooling rate of 30 K/s. To produce purely amorphous CF/PA6 cooling rates above 400 K/s are necessary.

The results for PA6 correlate well with findings of Brucato et al. [4] who investigated the cooling rate dependence of the crystallinity in PA6 and found a critical transition area between α- and γ-plateau at a cooling rate value of 10 K/s. Kolesov [8] demonstrated in Flash-DSC experiments a steady decrease of crystallization enthalpy between 0.01 K/s and 200 K/s which indicates a decrease in crystallinity from 36% (based on a 100% crystallization enthalpy of 241 J/g) to 0%. This indicates that cooling rates up to 150-200 K/s are necessary to produce pure amorphous PA6.

The presence of carbon fibres increases the crystallinity of PA6 slightly at cooling rates between 10 K/s and 100 K/s. This effect is also observed in literature: Feng [16] indicates an increased crystallinity of CF/PA6 and concluded that carbon fibres may work as nucleation agents. At high cooling rates above 100 K/s the crystallinity of neat PA6 and CF/PA6 is similar. A reduced influence of nano clay as nucleation agent was found by [15] for high cooling rates as well. An α-phase rich core region was not observed in the sample because of the higher thermal conductivity of CF/PA6. Nevertheless the results indicate that there is a likelihood that at lower cooling rates an α-phase may occur.

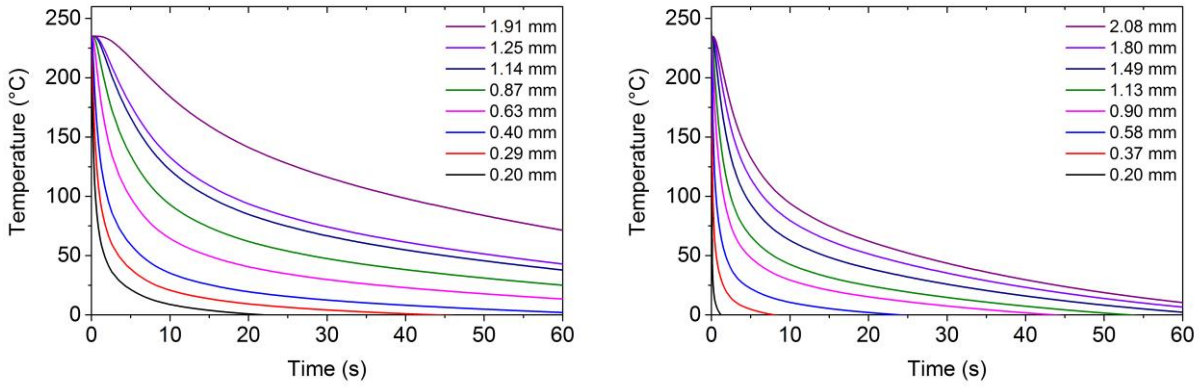

(a) PA6 (b) CF/PA6

Figure 5: Estimated temperature profiles at the investigated measurement depths.

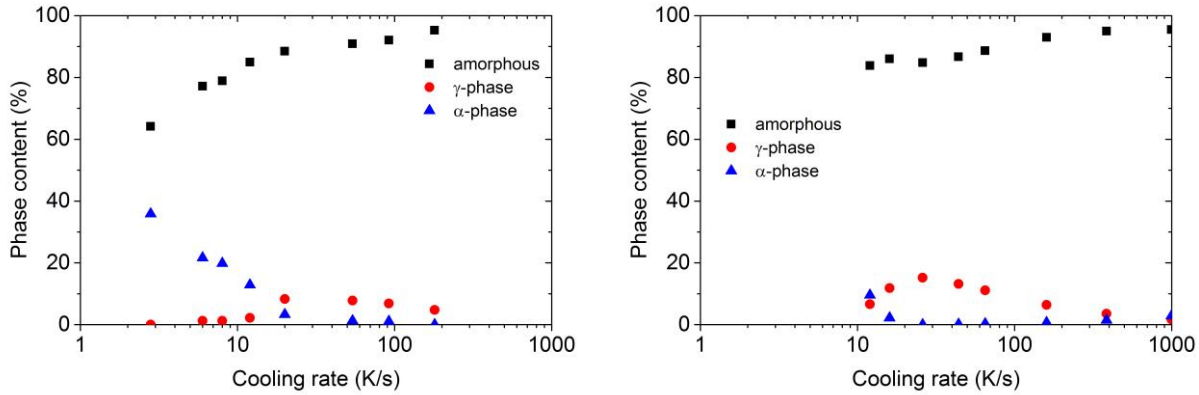

(a) PA6 (b) CF/PA6

Figure 6: Phase content of PA6 polymer in neat and carbon fibre reinforced samples as function of the estimated cooling rate at 135°C.

Therefore, the presence of carbon fibres may induce a strong skin-core morphology of CF/PA-6 samples in general: a strong increase in thermal conductivity leads to increased cooling rates at the surface during solidification and with this to a high γ-phase fraction. And the nucleation effect of carbon fibres at low cooling rates, which was observed by [16] leads to an increased α-phase fraction in the core region of a CF/PA-6 specimen.

4 CONCLUSIONS

The results of this study show the influence of carbon fibres on the crystallinity of Polyamide-6 at different cooling rates. Carbon fibre reinforced Polyamide-6 shows increased γ-phase fractions at cooling rates of ca. 30 K/s but only slight increase in the total amount of the crystalline fraction. At higher cooling rates the influence of carbon fibres on the crystallinity of Polyamide-6 is negligible.

Nevertheless, at moderate cooling rates the fibres may increase the metastable γ-phase fraction due to an increased thermal conductivity at cold surfaces. Therefore, a strong skin-core morphology would be expected for processing conditions similar to injection molding. Compared to neat Polyamide-6 the skin layer in the CF/PA-6 used in this study was found to increase by a factor of three.

ACKNOWLEDGEMENTS

We acknowledge the financial support of the German Federal Ministry for Education and Research (BMBF) for funding the project MAI Plast within the Leading-Edge cluster MAI Carbon.

REFERENCES

[1] Illers, V. K.-H. and Haberkorn, H. 1971. Schmelzverhalten, struktur und kristallinität von 6-polyamid. *Makromol. Chem.* 142, 1, 31–67.

[2] Illers, K.-H. 1978. Polymorphie, kristallinität und schmelzwärme von poly(ε-caprolactam), 2. Kalorimetrische untersuchungen. *Makromol. Chem.* 179, 2, 497–507.

[3] Roldan, L. G. and Kaufman, H. S. 1963. Crystallization of nylon 6. *J. Polym. Sci. B Polym. Lett.* 1, 11, 603–608.

[4] Brucato, V., Kiflie, Z., La Carrubba, V., and Piccarolo, S. 2009. The continuous cooling transformation (CCT) as a flexible tool to investigate polymer crystallization under processing conditions. *Adv. Polym. Technol.* 28, 2, 86–119.

[5] Cavallo, D., Gardella, L., Alfonso, G., Portale, G., Balzano, L., and Androsch, R. 2011. Effect of cooling rate on the crystal/mesophase polymorphism of polyamide 6. *Colloid Polym Sci* 289, 9, 1073-1079.

[6] Kyotani, M. and Mitsuhashi, S. 1972. Studies on crystalline forms of nylon 6. II. Crystallization from the melt. *J. Polym. Sci. A-2 Polym. Phys.* 10, 8, 1497–1508.

[7] Kyotani, M. 1975. Studies on crystalline forms of Nylon 6. III. Crystallization from the glassy state. *J. of Macromolecular Sc., Part B* 11, 4, 509–525.
[8] Kolesov, I., Mileva, D., Androsch, R., and Schick, C. 2011. Structure formation of polyamide 6 from the glassy state by fast scanning chip calorimetry. *Polymer* 52, 22, 5156–5165.
[9] Dencheva, N., Denchev, Z., Oliveira, M. J., and Funari, S. S. 2007. Relationship between crystalline structure and mechanical behavior in isotropic and oriented polyamide 6. *J. Appl. Polym. Sci.* 103, 4, 2242–2252.
[10] Shen, L., Phang, I. Y., and Liu, T. 2006. Nanoindentation studies on polymorphism of nylon 6. *Polymer Testing* 25, 2, 249–253.
[11] Ito, M., Mizuochi, K., and Kanamoto, T. 1998. Effects of crystalline forms on the deformation behaviour of nylon-6. *Polymer* 39, 19, 4593–4598.
[12] Lee, Y. and Porter, R. S. 1986. Crystallization of poly (etheretherketone)(PEEK) in carbon fiber composites. *Polymer Engineering & Science* 26, 9, 633–639.
[13] Velisaris, C. N. and Seferis, J. C. 1986. Crystallization kinetics of polyetheretherketone (peek) matrices. *Polym. Eng. Sci.* 26, 22, 1574–1581.
[14] Bessell, T. and Shortall, J. B. 1975. The crystallization and interfacial bond strength of nylon 6 at carbon and glass fibre surfaces. *J Mater Sci* 10, 12, 2035–2043.
[15] Fornes, T. and Paul, D. 2003. Crystallization behavior of nylon 6 nanocomposites. *Polymer* 44, 14, 3945–3961.
[16] Feng, N., Wang, X., and Wu, D. 2013. Surface modification of recycled carbon fiber and its reinforcement effect on nylon 6 composites: Mechanical properties, morphology and crystallization behaviors. *Current Applied Physics* 13, 9, 2038–2050.
[17] Murthy, N. S., Kagan, V. A., and Bray, R. G. 2002. Effect of melt temperature and skin-core morphology on the mechanical performance of nylon 6. *Polym. Eng. Sci.* 42, 5, 940–950.
[18] Brucato, V., Crippa, G., Piccarolo, S., and Titomanlio, G. 1991. Crystallization of polymer melts under fast cooling. I: Nucleated polyamide 6. *Polym. Eng. Sci.* 31, 19, 1411–1416.